FERROUS SMECTITES AND THE REDOX EVOLUTION OF EARLY MARS. J.G. Catalano[1], S.M. Chemtob[2], R.D. Nickerson[1], R.V. Morris[3], D.G. Agresti[4], [1]Washington Univ., St. Louis, MO (catalano@wustl.edu), [2]Temple Univ., Philadelphia, PA, [3]Johnson Space Center, Houston, TX, [4]Univ. of Alabama, Birmingham, AL.

Introduction: Ferric smectite clay minerals are a widely observed weathering product in the Noachian-aged basaltic crust of Mars [1]. The occurrence of Fe^{3+} in these clays, however, raises substantial questions about the redox state of early Mars. Earth was anoxic until the Great Oxidation Event (~2.4-2.2 Ga) [2], and it unclear when widespread surface oxidation occurred on Mars. As Noachian-aged smectites represent some of the earliest materials recording both fluid-rock interaction and redox state (through their structural Fe), they potentially may provide great insight into the redox evolution of early Mars. We have combined observational and theoretical evidence to explore formation and alteration pathways of iron-bearing smectites to constrain possible near-surface conditions during the Noachian.

Thermodynamic Predictions and Terrestrial Observations: Thermodynamic modeling [3] predicts that anoxic alteration of typical Martian basalt generates trioctahedral Fe(II)/Mg smectites clay minerals (**Fig. 1**). These models also predict that later oxidation generates Fe(III) smectites. Observations of terrestrial smectite compositions shows that those formed in anoxically-altered basaltic crust are mixed Fe-Mg trioctahedral smectites (**Fig. 2**), containing primary ferrous iron. Together, this shows that ferrous trioctahedral smectites are the expected alteration product of basalts before widespread surface oxidation occurred.

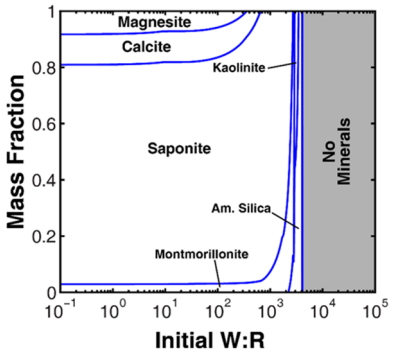

Figure 1: *Products of Adirondack basalt weathering under anoxic conditions by a fluid initially containing $10^{-2.5}$ molal H_2SO_4 at $P_{CO2} = 10^{-3}$ bar [3].*

Ferrous Smectite Synthesis and Characterization: Single-phase synthetic trioctahedral smectites [4] show systematic variations with composition in VNIR spectra (**Fig. 3**). Notably, Fe(II)-rich smectites show weak metal-OH bands and those with moderate Fe(II) contents have bands dominated by the Mg component. Hydrothermal basalt alteration yields Fe(II)-Mg smectites of similar composition and structure [5].

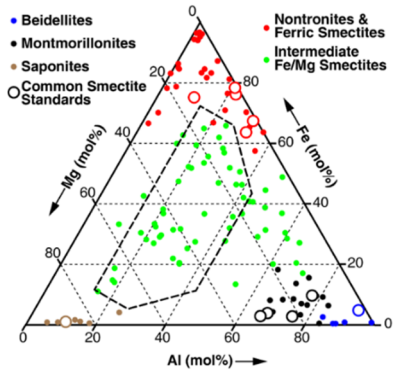

Figure 2: *Terrestrial smectite compositions; the box indicates clays from unoxidized altered oceanic crust.*

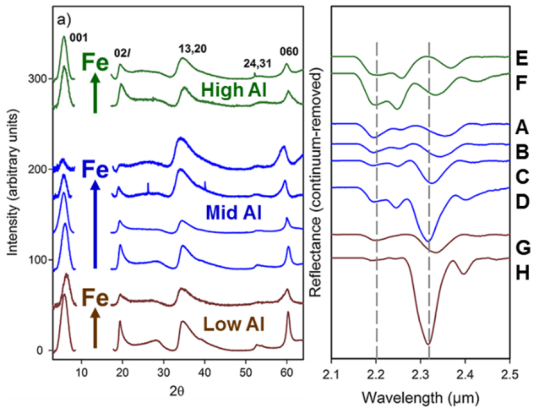

Figure 3: *XRD patterns (left) and VNIR spectra (right) of Fe(II)-Mg smectites of varying composition [4].*

Ferrous Smectite Oxidation: Experimental oxidation of Fe(II)-Mg smectites is rapid and nearly complete upon exposure to hydrogen peroxide. In contrast, dissolved oxygen yields only partial oxidation, with the extent of oxidation varying systematically with Fe(II) content (**Fig. 4**). Fe(II)-rich clays show substantial variations in XRD patterns and VNIR spectra upon oxidation, but those having <50% of octahedral sites filled

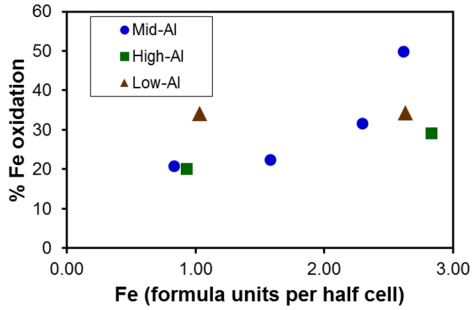

Figure 4: *Extent of Fe oxidation (determined by XANES spectroscopy) in Fe(II)-Mg smectites upon exposure to dissolved O_2 for 1 week.*

with Fe(II) show little change (**Fig. 5**). Recrystallization of the smectites resets the structure and allows for greater oxidation of iron by dissolved oxygen, with the clays progressing towards ferric smectites.

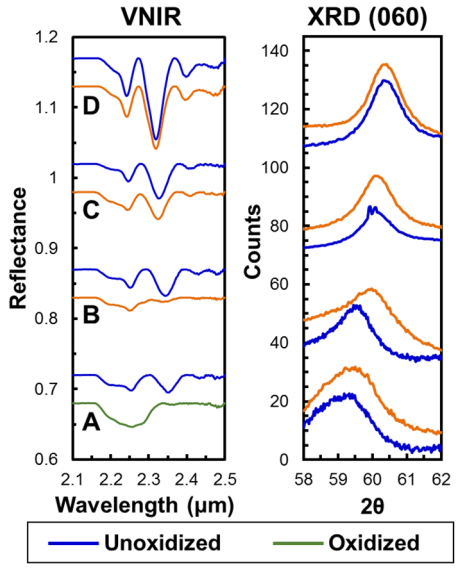

Figure 5: *VNIR spectra (left) and XRD patterns near the (060) reflection (right) of Fe(II)-Mg smectites subject to oxidation by dissolved O_2.*

Implications to Early Mars: This work shows that the ferric smectites observed on Mars today can be produced through initial formation of a ferrous smectite and later oxidation. Because oxidants on Mars are atmospherically derived [5] and exposure is thus generally limited to surface materials, it is possible that early ferrous smectites are still preserved in the subsurface.

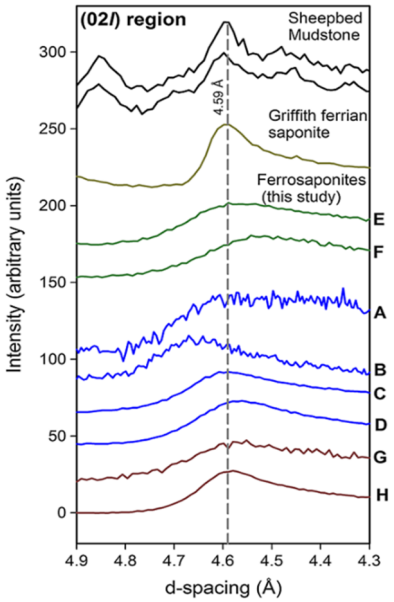

Figure 6: *Comparison of the (02l) features in XRD patterns of clays from the Sheepbed unit at Gale Crater to those of synthetic Fe(II)-Mg smectites [4].*

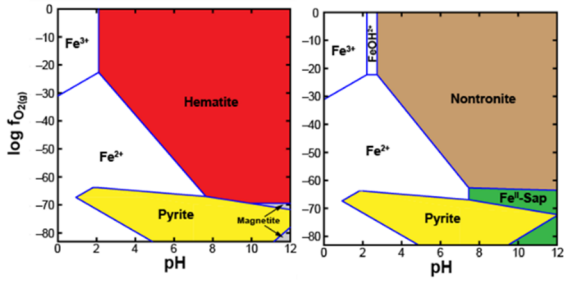

Figure 7: *Stability diagrams for Fe oxides (left) and smectites (right) at 25°C. Total Fe was 10^{-6} molal, total Ca^{2+} and SO_4^{2-} were each set to 10^{-3} molal and SiO_2, Al^{3+}, and Mg^{2+} activities were buffered by amorphous silica, montmorillonite, and Mg-saponite, respectively.*

Comparison of XRD features of synthetic Fe(II)-Mg smectites to those of clays from Gale Crater [6] show that these smectites need not contain any Fe(III). Thermodynamic stability calculations (**Fig. 7**) show that Fe(II)-bearing smectites are the stable clay phase in the presence of magnetite and iron sulfides found in the Sheepbed unit [6]. The mineralogy of these mudstones is thus compatible with an anoxic formation environment. Thermodynamic parameters were estimated for the mixed-valent Griffith ferrian saponite, which also has XRD features that well match those observed in the Sheepbed unit [7], but this mineral proved to be metastable with respect to Fe(II)-saponite and nontronite in the stability calculations. Further work is needed to assess the thermodynamic properties of this clay and determine its formation conditions.

Together, these studies show that Noachian-aged Fe-smectites are consistent with formation under anoxic conditions. Orbital observations at Mawrth Vallis and Nili Fossae show Fe/Mg smectite units overlain by leached horizons containing Al-phyllosilicates that are low in Fe oxides [8]. This sequence differs from what forms during oxic leaching on Earth [9]. Thus, widespread oxidation of the Martian surface post-dates Noachian clay formation and possibly even mudstone deposition in Gale Crater. Further subsurface exploration is needed to better constrain the redox evolution of Mars.

References: [1] Ehlmann B.L. and Edwards C.S. (2014) *AREPS* **42**, 291-315. [2] Lyons T.W. et al. (2014) *Nature* **506**, 307-315. [3] Catalano J.G. (2013) *JGR* **118**, 2124-2136. [4] Chemtob S.M. et al. (2015) *JGR* **120**, 1119-1140. [5] Nickerson R.D. et al. (2015) *LPS XLVI*, Abstract #2903 [5] Encrenaz T. et al. (2015) *A&A* **578**, A127. [6] Vaniman D.T. et al. (2014) *Science* **343**, 6169. [7] Treiman A.H. et al. (2014) *Amer. Miner.* **99**, 2234-2250. [8] Ehlmann B.L. et al. (2009) *JGR* **114**, E00D08. [9] Greenberger R.N. et al. (2012) *JGR* **117**, E00J12.